Mobile impurity in a two-leg bosonic ladder

Naushad Ahmad Kamar [1,2] Adrian Kantian [3,4] and Thierry Giamarchi [1]
[1]DQMP, University of Geneva, 24 Quai Ernest-Ansermet, 1211 Geneva, Switzerland
[2]Department of Physics and Astronomy, Michigan State University, East Lansing, Michigan 48824, USA
[3]Department of Physics and Astronomy, Uppsala University, Box 516, S-751 20 Uppsala, Sweden
[4]SUPA, Institute of Photonics and Quantum Sciences, Heriot-Watt University, Edinburgh EH14 4AS, United Kingdom

(Received 18 October 2023; accepted 18 July 2025; published 8 August 2025)

We study the dynamics of a mobile impurity in a two-leg bosonic ladder. The impurity moves both along and across the legs and interacts with a bath of interacting bosonic particles present in the ladder. We use both analytical (Tomonaga-Luttinger liquid) and numerical [Density Matrix Renormalization Group (DMRG)] methods to compute the Green's function of the impurity. We find that for a small impurity-bath interaction, the symmetric mode of the impurity effectively couples only to the gapless mode of the bath while the antisymmetric mode of the impurity couples to both gapped and gapless modes of the bath. We compute the time dependence of the Green's function of the impurity, for impurity created in either the antisymmetric or symmetric mode with a given momentum. The latter case leads to a decay as a power law below a critical momentum and exponential above, while the former case exhibits both power-law and exponential decay depending on the transverse tunneling of the impurity. We compare the DMRG results with analytical results using the linked cluster expansion and find good agreement. In addition, we use DMRG to extract the lifetime of the quasiparticle, when the Green's function decays exponentially. We also treat the case of an infinite bath-impurity coupling for which both the symmetric and antisymmetric modes are systematically affected. For this case, the impurity Green's function in the symmetric mode decays as a power law at zero momentum. The corresponding exponent increases with increasing transverse tunneling of the impurity. We compare our results with other impurity problems for which the motion of either the impurity or the bath is limited to a single chain. Finally, we comment on the consequences of our findings for experiments with the ultracold gases.

DOI: 10.1103/vh99-hdhh

I. INTRODUCTION

In a high-dimensional bath, a mobile impurity behaves as a free particle, with a renormalized mass and lifetime; this description of the impurity is known as a quasiparticle (QP) [1–4]. The QP description has been successfully applied to many problems from condensed matter to ultracold gases [5–7]. One classic example is the motion of an electron in the bath of phonons where the mass of the electron renormalizes and the electron behaves like a QP, known as a polaron.

However, it is known that several mechanisms can lead to a very different physics than simple quasiparticles. This is the case in the celebrated x-ray edge problem where the appearance of a static impurity induces an infinite number of excitations in the bath, leading to the famous Anderson orthogonality catastrophe [8,9]. Originally, the x-ray edge problem was observed for fermionic bath; it can also be extended to bosonic bath [9]. Similar physics occurs also in the Caldeira-Leggett problem where coupling to a bath can impede the tunneling of a macroscopic quantum variable [3,4]. Recently, similar phenomena were shown to drastically affect the motion of impurities moving in a one-dimensional (1D) bath of quantum interacting particles, leading to a motion quite different from a QP with a renormalized mass, namely, subdiffusion, and the Green's function of the impurity exhibiting a power-law decay for a wide range of momenta [10–16]. A part of this physics is due to the fact that in one dimension the recoil due to the motion of the impurity does not totally suppress the Anderson orthogonality catastrophe, contrarily to what happens in higher dimensions [17,18]. Thus, one of the questions of interest is how a mobile impurity will behave in a bath that has both transverse and horizontal extensions. This is a first step toward studying the dimensional crossover in the impurity dynamics. To answer these questions, the dynamics of a mobile impurity in the ladder bath has been recently investigated for a system for which the impurity moves only along the legs of the ladder [19] and in two decoupled chains where an impurity tunnels in both longitudinal and transverse directions [20,21]. For such systems, the impurity exhibits a similar class of dynamics as that of the 1D bath, but the power-law exponent becomes smaller in comparison to the one-dimensional bath.

The study of a mobile impurity in a quantum bath is not limited to theoretical studies, and experiments on the ultracold gases [22–25] provide in particular a platform to investigate such problem with a large flexibility and control on the impurity and the bath.

In this work, we address the dynamics of a mobile impurity in a two-leg bosonic ladder, with the impurity being able to tunnel between the two legs. Compared to the single-chain case, where the impurity was restricted to a 1D motion, we can expect that, in the present setup, the recoil effects could be more pronounced than in the strictly 1D case [26]. Another way to study such a problem is to consider the leg index as some "spin" index for both the bath and the impurity. In such a description, the present problem would be a generalization of the Kondo problem (by opposition to the x-ray edge one with a featureless impurity) but with the possibility of motion of the impurity. This poses the question of the subtle coupling of the internal and center-of-mass degrees of freedom.

We study this problem using the numerical method, i.e., time-dependent density matrix renormalization group (t-DMRG) [27,28] and analytical methods such as Tomonaga-Luttinger liquid (TLL) [9,29] and linked cluster expansion (LCE) [30]. The t-DMRG allows us to access the impurity dynamics from weak to strong interactions with the bath, while LCE describes the impurity dynamics in the weak coupling limit. We compare our results with previous studies on the impurity dynamics in the one-dimensional bath [31] and the ladder bath [19].

The plan of the paper is as follows: In Sec. II, we describe the model on the lattice and in the continuum limit, its bosonization representation, and various observables. In Sec. III, we describe the analytical expression of the observables by using bosonization and the LCE. In Sec. IV, we present the numerical t-DMRG [27,28], analysis of this problem, and the results for the Green's function of the impurity. Section V discusses these results both in connection with the one-dimensional motion of an impurity in a ladder's results and in view of the possible extensions. Finally, Sec. VI concludes the paper and presents some perspectives in connection with experiments. The analytical expression of the Green's function is given in Appendix.

II. MOBILE IMPURITY IN A TWO-LEG BOSONIC LADDER

A. Model

We consider a mobile impurity moving in a two-leg bosonic ladder in both horizontal and transverse directions. The model we consider is depicted in Fig. 1.

The full Hamiltonian is given by

$$H = H_K + H_{\rm lad} + U_{1\rm imp}\sum_{j=1}^{L}\rho_{1,j}\rho_{\rm imp,1,j} + U_{2\rm imp}\sum_{j=1}^{L}\rho_{2,j}\rho_{\rm imp,2,j}, \tag{1}$$

where $U_{1\rm imp}$, $U_{2\rm imp}$, and L are the interaction strength between the particles in leg 1 and in leg 2 with the impurity, and the ladder size along the longitudinal direction, respectively. Also, $\rho_{1,j}$, $\rho_{2,j}$, $\rho_{\rm imp,1,j}$, and $\rho_{\rm imp,2,j}$ denote the density operator of the bath in leg 1 and leg 2, and the density operator of the impurity in leg 1 and leg 2, respectively. We consider $U_{1\rm imp} = U_{2\rm imp} = U$.

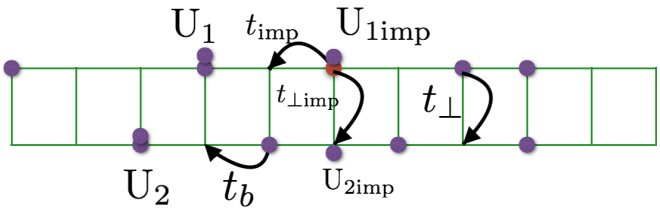

FIG. 1. Impurity in a two-leg bosonic ladder. The blue solid circles represent the bath particles and the red circle represents the impurity. The bath particles move along the legs (resp. between the legs) with hopping t_b (resp. $t_\perp$) (see text). The impurity moves in both longitudinal and transverse directions with amplitudes $t_{\rm imp}$ and $t_{\perp\rm imp}$ (see text), respectively. The impurity and the bath particles interact by the contact interactions $U_{1\rm imp}$ and $U_{2\rm imp}$ in leg 1 and leg 2, respectively.

The impurity kinetic energy is given by the tight-binding Hamiltonian

$$H_K = -t_{\rm imp}\sum_{j=1}^{L-1}(d^\dagger_{1,j+1}d_{1,j} + d^\dagger_{2,j+1}d_{2,j} + \text{H.c.}) - t_{\perp\rm imp}\sum_{j=1}^{L}(d^\dagger_{1,j}d_{2,j} + \text{H.c.}). \tag{2}$$

We diagonalize H_K by using symmetric and antisymmetric combinations of $d_{1,j}$ and $d_{2,j}$, and H_K can be reexpressed as

$$H_K = \sum_q \epsilon_s(q)d^\dagger_{s,q}d_{s,q} + \epsilon_a(q)d^\dagger_{a,q}d_{a,q}, \tag{3}$$

where $d_{\gamma,j}$ ($d^\dagger_{\gamma,j}$) are the destruction (creation) operators of the impurity on site j in leg $\gamma = 1, 2$, $d_{s,q} = (d_{1,q} + d_{2,q})/\sqrt{2}$, $d_{a,q} = (d_{1,q} - d_{2,q})/\sqrt{2}$, $\epsilon_a(q) = -2t_{\rm imp}\cos(q) + t_{\perp\rm imp}$, and $\epsilon_s(q) = -2t_{\rm imp}\cos(q) - t_{\perp\rm imp}$. The density of the impurity $\rho_{{\rm imp},\gamma,j}$ and Fourier transformation of $d_{\gamma,j}$ are defined as

$$\rho_{{\rm imp},\gamma,j} = d^\dagger_{\gamma,j}d_{\gamma,j}, \qquad \hat{d}_{\gamma,q} = \sum_j e^{iqr_j}d_{\gamma,j}, \tag{4}$$

where $r_j = aj$, and $a = 1$ is lattice constant. The ladder Hamiltonian $H_{\rm lad}$ is given by

$$H_{\rm lad} = H_1^0 + H_2^0 - t_\perp\sum_{j=1}^{L}(b^\dagger_{1,j}b_{2,j} + \text{H.c.}), \tag{5}$$

where $b_{\gamma,j}$ ($b^\dagger_{\gamma,j}$) are the destruction (creation) operators for a boson in the bath on chain γ and site j. The operator b obeys the usual bosonic commutation relation rules. The single-chain Hamiltonian is the Bose-Hubbard one:

$$H_i^0 = -t_b\sum_{j=1}^{L-1}(b^\dagger_{i,j+1}b_{i,j} + \text{H.c.}) + \frac{U_i}{2}\sum_{j=1}^{L}\rho_{i,j}(\rho_{i,j} - 1) - \mu_i\sum_j\rho_{i,j}, \tag{6}$$

where $\rho_{\gamma,j} = b^\dagger_{\gamma,j} b_{\gamma,j}$ is density operator of the ladder in leg γ and site j. Equation (1) is convenient for the numerical study. In order to make connection with the field theory analysis, we can also consider the same problem in a continuum. In that case, the Hamiltonian becomes

$$H = \frac{P^2}{2M} - t_{\perp \mathrm{imp}}(|1\rangle\langle 2| + |2\rangle\langle 1|) + H_{\mathrm{lad}} + U(\rho_1(X)|1\rangle\langle 1| + \rho_2(X)|2\rangle\langle 2|), \quad (7)$$

where X and P are the position and momentum operators of the impurity, respectively, and $\rho_\gamma(X)$ is density operator of the bath at position X in leg γ of the ladder. The basis sets $|1\rangle$ and $|2\rangle$ represent the chain index of the ladder, and they form a complete basis ($|1\rangle\langle 1| + |2\rangle\langle 2| = I$, where I is a 2×2 identity matrix). The last two terms in Eq. (7) arise from the fact that the impurity density operators in leg 1 and leg 2 are $\rho_{\mathrm{imp},1}(x) = \delta(x - X)|1\rangle\langle 1|$ and $\rho_{\mathrm{imp},2}(x) = \delta(x - X)|2\rangle\langle 2|$, respectively.

The ladder Hamiltonian in Eq. (5) in the continuum becomes

$$H_{\mathrm{lad}} = H_1^0 + H_2^0 - t_\perp \int dx(\psi_1^\dagger(x)\psi_2(x) + \mathrm{H.c.}), \quad (8)$$

and the single-chain Hamiltonian is

$$H_i^0 = \frac{1}{2m}\int dx|\nabla\psi_i(x)|^2 + \frac{U_i}{2}\int dx\rho_i(x)^2 - \mu_i \int dx\rho_i(x), \quad (9)$$

where m is the mass of the bosons, μ_i is the chemical potential, and U_i is the intrachain interaction.

B. Observables

To characterize the dynamics of the impurity in the ladder, we mostly focus on the Green's function of the impurity. We study it at zero temperature both analytically and numerically via DMRG. Compared to the case [19] where the impurity was confined to a single chain, it is now necessary to introduce two independent Green's functions for the impurity. The Green's functions are in the chain basis:

$$G_{\alpha\beta}(p,t) = \langle \hat{d}_{\alpha,p}(t)\hat{d}^\dagger_{\beta,p}(t=0)\rangle, \quad (10)$$

where α and β can take the values 1 and 2 corresponding to the chain index and $\langle\cdots\rangle$ denotes the average in the ground state of the bath, and with zero impurities present. $O(t)$ denotes the usual Heisenberg time evolution of the operator:

$$O(t) = e^{iHt} O e^{-iHt}. \quad (11)$$

By symmetry, we can restrict ourselves to $G_{11}(p,t)$ and $G_{12}(p,t)$. The two other Green's functions are simply related to Eq. (10) by $G_{22}(p,t) = G_{11}(p,t)$ and $G_{12}(p,t) = G_{21}(p,t)$.

Instead of using the chain basis, it can be more convenient to use the symmetric and antisymmetric operators of the impurity, leading to the two Green's functions:

$$G_s(p,t) = \langle \hat{d}_{s,p}(t)\hat{d}^\dagger_{s,p}(t=0)\rangle,$$
$$G_a(p,t) = \langle \hat{d}_{a,p}(t)\hat{d}^\dagger_{a,p}(t=0)\rangle. \quad (12)$$

One has $G_s(p,t) = G_{11}(p,t) + G_{12}(p,t)$ and $G_a(p,t) = G_{11}(p,t) - G_{12}(p,t)$.

C. Bosonization representation

To deal with the Hamiltonian defined in the previous section, we use the fields $\theta_\alpha(x)$ and $\phi_\alpha(x)$ [9] for chain $\alpha = 1, 2$, which are related to the field operators of the system via

$$\rho_\alpha(x) = \rho_{0,\alpha} - \frac{\nabla\phi_\alpha(x)}{\pi} + \rho_{0,\alpha}\sum_{p\neq 0} e^{2ip(\pi\rho_{0,\alpha}x - \phi_\alpha(x))}, \quad (13)$$

where $\rho_{0,\alpha}$ is the average density on the chain $\alpha = 1, 2$. For equivalent upper and lower legs of the ladder, we can take $\rho_{0,1} = \rho_{0,2} = \rho_0$. The creation operator of a particle in the bath in terms of θ and ϕ is given to lowest order by

$$\psi^\dagger_\alpha(x) = \rho_{0,\alpha}^{1/2} e^{-i\theta_\alpha(x)}. \quad (14)$$

The conjugate field operators $\phi_{1,2}$ and $\theta_{1,2}$ obey

$$\left[\phi(x_1), \frac{\nabla\theta(x_2)}{\pi}\right] = i\delta(x_1 - x_2). \quad (15)$$

Using the bosonization framework, the Hamiltonian of the ladder is given by

$$H_{\mathrm{lad}} = H_s + H_a, \quad (16)$$

with

$$H_s = \frac{1}{2\pi}\int dx\left[u_s K_s(\partial_x\theta_s)^2 + \frac{u_s}{K_s}(\partial_x\phi_s)^2\right],$$
$$H_a = \frac{1}{2\pi}\int dx\left[u_a K_a(\partial_x\theta_a)^2 + \frac{u_a}{K_a}(\partial_x\phi_a)^2\right] - 2\rho_0 t_\perp \int dx\cos(\sqrt{2}\theta_a(x)), \quad (17)$$

and

$$\theta_{s,a} = \frac{\theta_1 \pm \theta_2}{\sqrt{2}},$$
$$\phi_{s,a} = \frac{\phi_1 \pm \phi_2}{\sqrt{2}}. \quad (18)$$

$K_{s,a}$ and $u_{s,a}$ are known as Luttinger parameters and control the properties of the bosonic ladder. The cosine term [9,19] opens a gap Δ_a in the antisymmetric sector when $K_a > 1/4$. This massive phase for the antisymmetric mode signals the existence of phase coherence across the two legs of the ladder, with exponentially decreasing correlations for the antisymmetric density-density correlations. The symmetric sector is described by the usual TLL Hamiltonian, and has power-law correlations. A numerical calculation of the TLL parameters for the massless phase can be found in Ref. [32].

III. ANALYTICAL SOLUTION FOR WEAK COUPLING ($U \ll \Delta_a$)

Let us now investigate the full Hamiltonian in Eq. (7) [or Eq. (1)] to compute the Green's function of the impurity (10).

Using Eq. (13), the interaction term H_{coup} with the impurity in terms of the d_s and d_a becomes

$$H_{\text{coup}} = \frac{U}{2}\int dx(\rho_1(x)+\rho_2(x))(d_s(x)^\dagger d_s(x)+d_a(x)^\dagger d_a(x)) + \frac{U}{2}\int dx(\rho_1(x)-\rho_2(x))(d_s(x)^\dagger d_a(x)+\text{H.c.}), \tag{19}$$

which leads to the expression, in terms of the symmetric and antisymmetric modes of the bath,

$$\begin{aligned} H_{\text{coup}} = {} & \frac{-U}{\sqrt{2}\pi}\int dx\nabla\phi_s(x)(d_s(x)^\dagger d_s(x)+d_a(x)^\dagger d_a(x)) \\ & -\frac{U}{\sqrt{2}\pi}\int dx\nabla\phi_a(x)(d_s(x)^\dagger d_a(x)+\text{H.c.}) \\ & +\frac{U\rho_0}{2}\int dx\cos(2\pi\rho_0 x-\sqrt{2}\phi_s)\cos(\sqrt{2}\phi_a) \\ & \times(d_s(x)^\dagger d_s(x)+d_a(x)^\dagger d_a(x)) \\ & -\frac{U\rho_0}{2}\int dx\sin(2\pi\rho_0 x-\sqrt{2}\phi_s)\sin(\sqrt{2}\phi_a) \\ & \times(d_s(x)^\dagger d_a(x)+\text{H.c.}). \end{aligned} \tag{20}$$

Since the field θ_a is ordered for $K_a > 1/4$, the correlation functions corresponding to its dual field ϕ_a will be exponentially suppressed. Thus, for $U \ll \Delta_a$, we can drop the cosine and sine terms in Eq. (20), and finally in weak coupling regime, Eq. (20) can be expressed as

$$\begin{aligned} H_{\text{coup}} = {} & \frac{-U}{\sqrt{2}\pi}\int dx\nabla\phi_s(x)(d_s(x)^\dagger d_s(x)+d_a(x)^\dagger d_a(x)) \\ & -\frac{U}{\sqrt{2}\pi}\int dx\nabla\phi_a(x)(d_s(x)^\dagger d_a(x)+\text{H.c.}). \end{aligned} \tag{21}$$

Note that we have kept in Eq. (21) only the most relevant term, which for bosons is the forward scattering on the symmetric and antisymmetric modes of the bath. In Eq. (21), the impurity-bath coupling U is distributed on both symmetric and antisymmetric modes of the bath with an effective interaction $U/\sqrt{2}$.

To compute the Green's functions, we use the same approach as in Ref. [19], namely, the linked cluster expansion [10,26,31]. The calculation is detailed in Appendix and gives the asymptotic behavior of the impurity Green's function (10) for $2t_{\perp\text{imp}} > \Delta_a\sqrt{2u_a\pi}/\sqrt{K_a}$ as

$$\begin{aligned} |G_s(0,t)| &\simeq \left(\frac{1}{t}\right)^\alpha, \\ |G_a(0,t)| &\simeq e^{-A_2U^2\pi t}\left(\frac{1}{t}\right)^\alpha, \end{aligned} \tag{22}$$

and for $2t_{\perp\text{imp}} < \Delta_a\sqrt{2u_a\pi}/\sqrt{K_a}$

$$\begin{aligned} |G_s(0,t)| &\simeq \left(\frac{1}{t}\right)^\alpha, \\ |G_a(0,t)| &\simeq \left(\frac{1}{t}\right)^\alpha, \end{aligned} \tag{23}$$

where $\alpha = K_sU^2/4\pi^2u_s^2$, and $K_s = 0.835$, $u_s = 1.86$, for $t_b = t_\perp = 1$, $U_1 = U_2 = \infty$, $\rho_0 = 1/3$ [32], and

$$A_2 \simeq \frac{K_a}{4u_a\pi^2}\frac{\left(u_a^2q_-^2+\tilde{\Delta}^2\right)}{q_-\left(2t_{\text{imp}}\sqrt{u_a^2q_-^2+\tilde{\Delta}^2}+u_a^2\right)}, \tag{24}$$

where q_- and $\tilde{\Delta}$ are expressed in Appendix. In our LCE calculation, we also find that for $2t_{\perp\text{imp}} < \Delta_a\sqrt{2u_a\pi}/\sqrt{K_a}$, Green's function in both symmetric and antisymmetric sectors decays as a power law [see Eq. (22)] at $p = 0$. This is an emergent effect of the ladder bath and transverse tunneling $t_{\perp\text{imp}}$ on the dynamics of the impurity. For decoupled chains ($\Delta_a = 0$) [20], the impurity Green's function decays as power law and exponentially in the symmetric and antisymmetric sectors at any finite transverse tunneling of the impurity, respectively; this behavior is also reproduced in Eq. (22).

For a weak repulsion between the impurity and the bath and $2t_{\perp\text{imp}} > \Delta_a\sqrt{2u_a\pi}/\sqrt{K_a}$, we thus find that the Green's function in the symmetric mode decays as a power law with time as was the case with an impurity confined to a single chain [19]. In the antisymmetric mode, on the other hand, it decays exponentially.

IV. NUMERICAL SOLUTION

Analyzing the regime $U \gg \Delta_a$ is much more involved since now excitations across the antisymmetric gap can be created. We thus turn to a numerical analysis of this problem.

A. Method

We use time-dependent DMRG [33] to compute the Green's function of the impurity, and we follow the method described in Refs. [19,31,34]. For completeness, let us recall the method, which is described below.

We map the ladder-impurity problem to a one-dimensional problem by a supercell approach. We denote bath particles in leg 1 and leg 2 by B and C, the impurity in leg 1 and leg 2 by A and D, and the total number of bath particles and number of impurity are conserved separately. The local dimension of Hilbert space for A, B, C, and D is two for hardcore bosons; hence, the dimension of local Hilbert space of supercell (A, B, C, and D) is $2\times2\times2\times2 = 16$. We compute the Green's function of the impurity in the ground state of the ladder. The ground state ($|GS\rangle$) is computed using DMRG. The Green's functions $G_{11}(x,t)(G_{12}(x,t))$ of the impurity in Heisenberg picture are given by

$$\begin{aligned} G_{11}(x,t) &= e^{iE_{\text{GS}}t}\langle GS|d_{1,\frac{L+1}{2}-x}e^{-iHt}d^\dagger_{1,\frac{L+1}{2}}|GS\rangle, \\ G_{12}(x,t) &= e^{iE_{\text{GS}}t}\langle GS|d_{2,\frac{L+1}{2}-x}e^{-iHt}d^\dagger_{1,\frac{L+1}{2}}|GS\rangle, \end{aligned} \tag{25}$$

where E_{GS} is ground-state energy of the bath. We compute $e^{-iHt}d^\dagger_{1,\frac{L+1}{2}}|GS\rangle$ using t-DMRG and $\langle GS|d_{2,\frac{L+1}{2}-x}$ ($\langle GS|d_{1,\frac{L+1}{2}-x}$) are computed using DMRG. By using $G_{11}(x,t)$ and $G_{12}(x,t)$, we compute $G_s(x,t) = G_{11}(x,t)+G_{12}(x,t)$ and $G_a(x,t) = G_{11}(x,t)-G_{12}(x,t)$. For the numerical calculation, we have used a bath of hardcore bosons at a density of $\rho_0 = 1/3$. This choice avoids the Mott-insulating phase that the ladder's symmetric mode

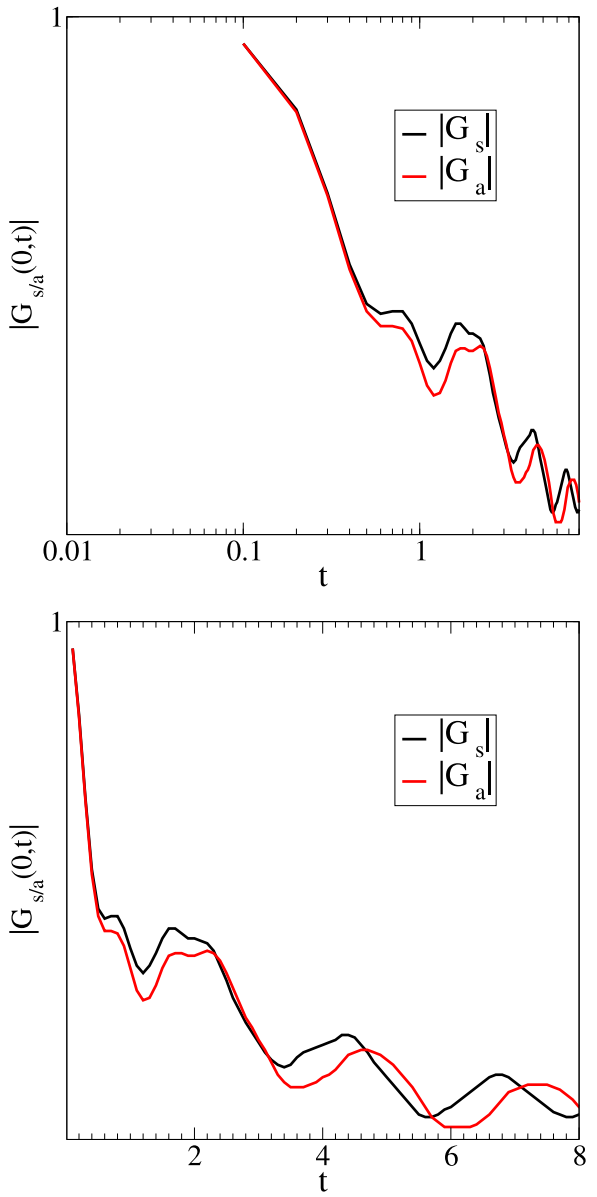

FIG. 2. Modulus of the impurity Green's function at $p = 0$ in the symmetric and antisymmetric sectors, shown on log-log (upper panel) and semilog (lower panel) scales as a function of time for a hardcore bosonic bath. Simulation parameters are $t_{\rm imp} = t_{\rm b} = 1$, $t_\perp = 1.0$, $U = 1.0$, $t_{\perp{\rm imp}} = 0.5$, and momentum $p = 0$. At small $t_{\perp{\rm imp}} = 0.5$, the Green's function decays as a power law in both sectors.

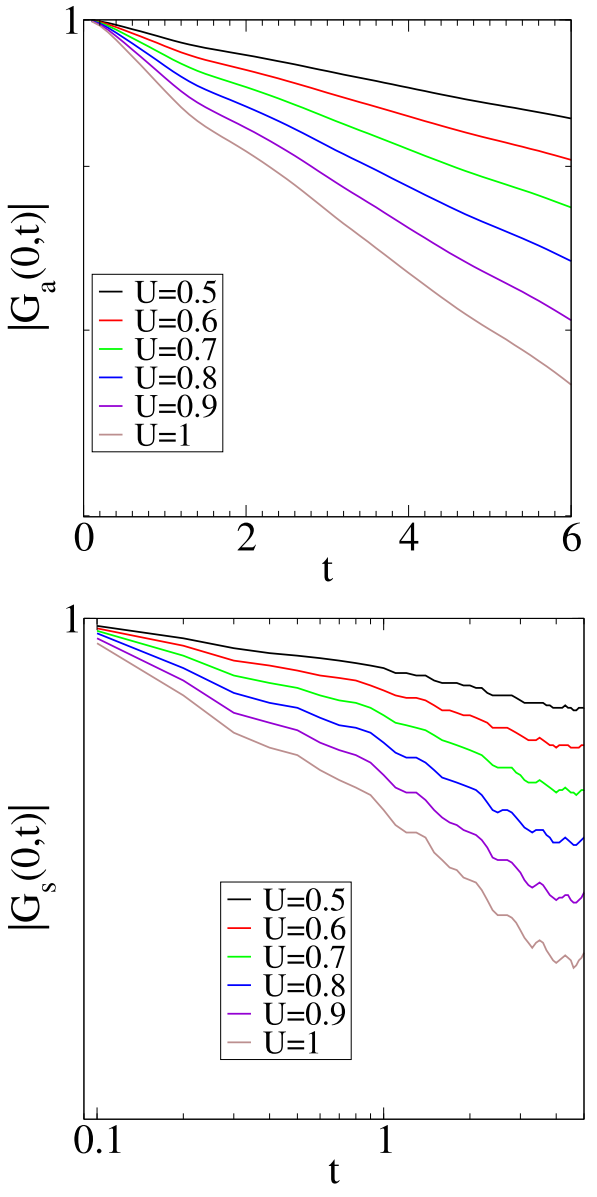

FIG. 3. The modulus of the Green's function of the impurity in antisymmetric (upper panel) and symmetric sectors (lower panel) as a function of time for hardcore bosonic bath at $t_{\rm imp} = t_{\rm b} = 1$, $t_\perp = 1$, U runs from 0.5 to 1, $t_{\perp{\rm imp}} = 3$, and $p = 0$. The upper panel depicted on semilog scale shows a linear behavior, while lower panel shows a linear behavior on log-log scale.

might enter at commensurate density [32]. We have used a bond dimension $\chi = 400$ to compute the Green's function in a reasonable time. We chose Hamiltonian parameters $t_\perp = t_b = t_{\rm imp} = 1, U_1 = U_2 = \infty$, and various values of $t_{\perp{\rm imp}}$ and U. We fix the size of the system to $L = 101$ sites per leg.

B. Zero-momentum regime

We show the Green's function of the impurity in the antisymmetric and symmetric modes $|G_a(p,t)|$, $|G_s(p,t)|$ at momentum $p = 0$ in Figs. 2 and 3 on semilog and log-log scales; we find that $|G_s(0,t)|$ decays as a power law, which is similar to one observed in one-dimensional motion of the impurity in a two-leg bosonic ladder [19]. However, the Green's function of the impurity in the antisymmetric mode shows a power-law decay at small $t_{\perp{\rm imp}} = 0.5$ as shown in Fig. 2, which is in agreement with our LCE findings, while for large $t_{\perp{\rm imp}} = 3.0$, it shows an exponential decay (shown in Fig. 3).

For the parameters used in these two figures, the gap in the antisymmetric sector is $\Delta_a = 0.33 t_b$. This value of the impurity-bath interaction corresponds to the regime of weak coupling for which a comparison with the analytical results of Sec. III is meaningful. The comparison of the numerical results with the analytical results (22) is shown in Fig. 4.

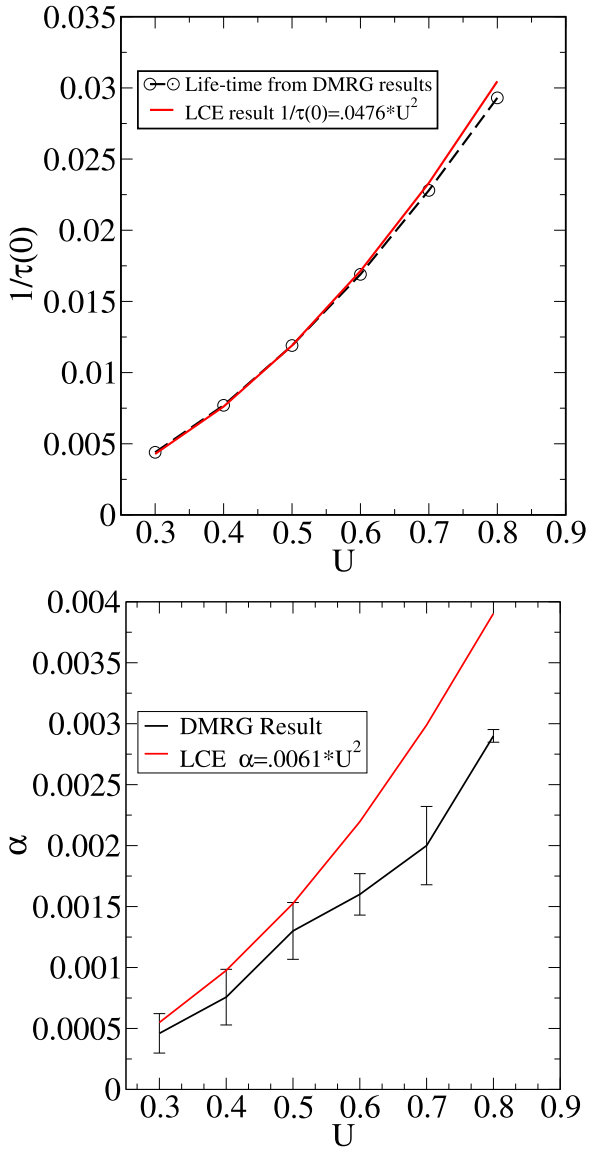

FIG. 4. Inverse lifetime of the impurity in antisymmetric sector (upper panel) and power-law exponent (lower panel) in the symmetric sector at $t_{\rm imp} = t_{\rm b} = 1$, $t_\perp = 1$, and $t_{\perp{\rm imp}} = 3$ as a function of U at zero momentum. The black lines are numerical results and the red lines are LCE results; both numerical and analytical results show a nice agreement for small U.

The numerical analysis thus fully confirms that in this regime $G_s(0,t)$ and $G_a(0,t)$ decay as power law and exponentially, respectively, for large $t_{\perp{\rm imp}} = 3$. To further analyze the data, we fit the numerical results to the form

$$|G_a(p=0,t)| \propto \exp(-t/\tau(0))$$
$$|G_s(p=0,t)| \propto \left(\frac{1}{t}\right)^{\alpha}. \tag{26}$$

1. *Small* U

To analyze the data, we use the analytical estimates of Sec. III, which suggest a power law and an exponential decay of the Green's function of the symmetric and the antisymmetric mode, respectively, at large $t_{\perp{\rm imp}}$.

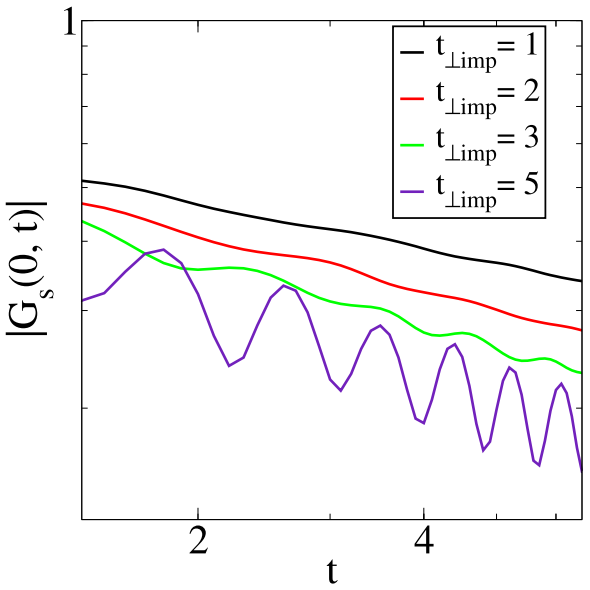

FIG. 5. Modulus of the Green's function of the impurity (see text) $|G_s(p,t)|$ at momentum $p = 0$. Parameters for the intrachain hopping, interchain hopping (for the ladder), impurity hopping, impurity-bath interaction, and impurity transverse tunneling in the ladder are $t_b = 1$, $t_\perp = 1$, $t_{\rm imp} = 1$, $U = \infty$, and $t_{\perp{\rm imp}} = 1, 2, 3,$ and 5, respectively.

We fit the numerical data with the LCE result at $p = 0$ and they agree very well with numerical results. The numerical and analytical results for G_a and G_s are shown in Fig. 4.

2. *Hardcore bath-impurity repulsion*

In the case of $U \to \infty$, $|G_s(p,t)|$ is plotted on the log-log scale in Fig. 5 for different values of $t_{\perp{\rm imp}}$ at $p = 0$. As shown, $|G_s(p,t)|$ decays as a power law, and the power-law exponent as a function of $t_{\perp{\rm imp}}$ is depicted in Fig. 6. The power-law exponent increases as a function of $t_{\perp{\rm imp}}$. For a small $t_{\perp{\rm imp}}$, the exponent is similar to the one observed for the purely one-dimensional motion of an impurity in a two-leg ladder bath [19], while for a large $t_{\perp{\rm imp}}$, it is similar to the motion of an impurity in a one-dimensional bath [14,31].

C. Green's function at finite momentum

As we have seen previously that the Green's function decays as a power law in the symmetric mode and exponentially in the antisymmetric mode at $p = 0$, now we turn on finite momentum. The Green's functions $|G_s(p,t)|$ and $|G_a(p,t)|$ for finite momentum are shown in Figs. 7 and 8, respectively, for various momenta p of the impurity. We find that $|G_s(p,t)|$ decays as power law below $p = 0.3\pi$. Beyond $p = 0.3\pi$, it decays exponentially and the impurity in the symmetric mode enters into a QP regime. An analogous crossover has been established in the one-dimensional motion of an impurity in a one-dimensional bath [31] and two-leg bosonic ladder bath [19,34].

The crossover depends on the TLL characteristics of the bath in the symmetric sector, namely, the velocity of sound u_s in the ladder and the TLL parameter K_s. Using the values

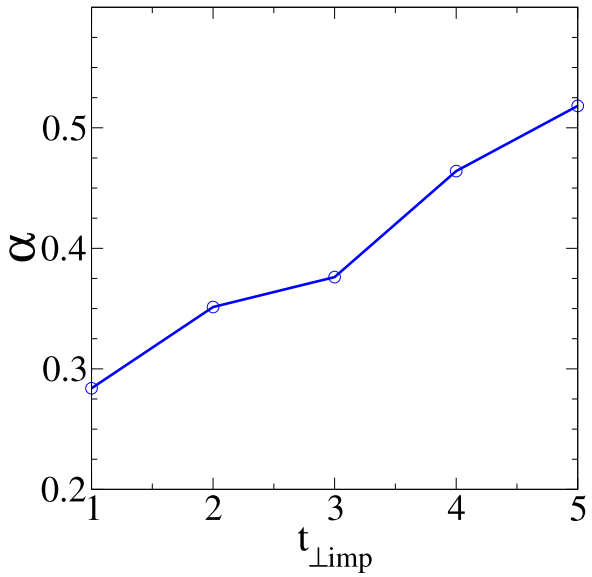

FIG. 6. Power-law exponent of the symmetric Green's function of the impurity with a hardcore repulsion with the bath of hardcore bosons at filling 1/3 as a function of $t_{\perp\text{imp}}$ at $t_{\text{imp}} = 1$, $U \to \infty$, and $p = 0$. Circles are the numerical data for $\chi = 400$ and the line is a guide to the eyes.

extracted from Ref. [32], we get

$$p^* = \frac{u_s}{2t_{\text{imp}}a^2} = 0.93, \tag{27}$$

which is in reasonably good agreement with the observed change of behavior in Fig. 7.

Beyond $p = p^*$ and for small U, the Green's function decays exponentially, the impurity behaves like a QP, and the Green's function of the impurity in terms of lifetime $\tau(p)$ is given by

$$|G_s(p,t)| = \exp(-t/\tau(p)). \tag{28}$$

In the top panel of Fig. 9, we plot the inverse of lifetime $1/\tau(p)$ in the symmetric mode of the impurity, defined in Eq. (28) of the QP as a function of p for interaction $U = 1, t_{\perp\text{imp}} = 3$. As can be expected, $1/\tau(p)$ increases with increasing p.

In Fig. 8, we have shown $|G_a(p,t)|$ on semilog and log-log scales; we find that $|G_a(p,t)|$ decays exponentially for all momenta at large $t_{\perp\text{imp}} = 3.0$, and the impurity in the antisymmetric mode behaves like a QP. In the bottom panel of Fig. 9, we have shown the inverse lifetime as a function p; it shows a nonmonotonic behavior but overall increases with increasing p.

In Fig. 10, we have summarized the results for small impurity-bath coupling.

V. DISCUSSION

Our findings suggest that the impurity exhibits very different dynamics in the ladder due to its motion in both the horizontal and transverse directions, compared to what is observed in the one-dimensional motion of an impurity in a ladder and a one-dimensional bath.

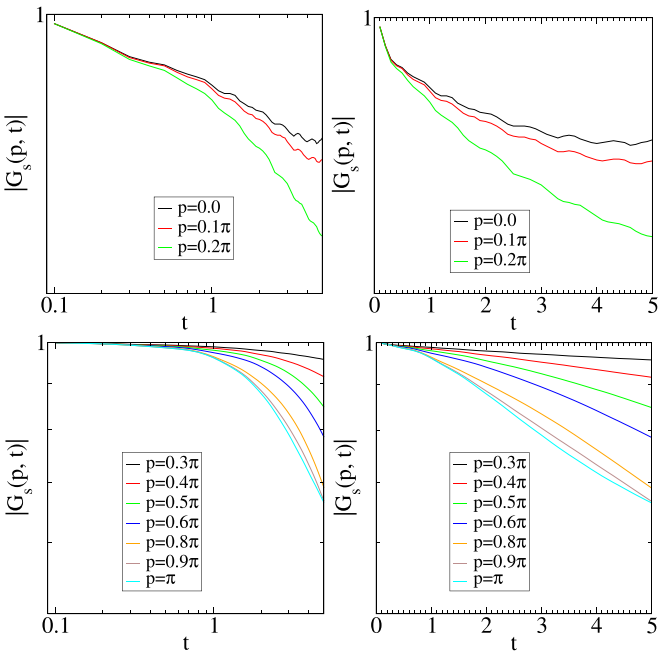

FIG. 7. Modulus of the Green's function of the impurity in the symmetric sector (see text) $|G_s(p,t)|$ at different momenta p (cf. legend) for the impurity. The Hamiltonian parameters are $t_b = 1$, $t_\perp = 1, t_{\text{imp}} = 1, t_{\perp\text{imp}} = 3$, and $U = 1.0$ on log-log scale (left panel) and semilog scale (right panel). We observe a linear behavior on log-log scale for small momenta ($p = 0 - 0.2\pi$) and linear behavior for large momenta $p = 0.3\pi - \pi$ on semilog scale.

Let us first discuss the weak interaction limit. Initially, both the symmetric and antisymmetric modes of the impurity couple to both the gapless and gapped modes of the bath, but our numerical and analytical findings suggest that in the long-time limit, the impurity in the antisymmetric sector effectively couples to both gapped and gapless modes of the bath, and the impurity in the symmetric mode couples to the gapless mode of the bath with an effective interaction $U/\sqrt{2}$ [see Eq. (21)]. We have performed an LCE calculation at zero momentum by using the effective coupling between the impurity and the

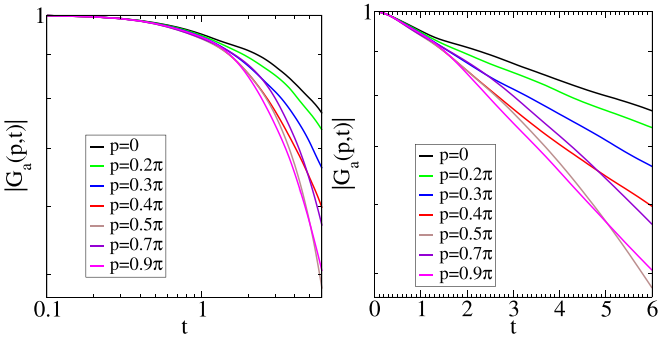

FIG. 8. Modulus of the Green's function of the impurity in antisymmetric sector (see text) $|G_a(p,t)|$ at different momenta p (shown in inset) for the impurity. The Hamiltonian parameters are $t_b = 1$, $t_\perp = 1, t_{\text{imp}} = 1, t_{\perp\text{imp}} = 3$, and $U = 1.0$ on log-log scale (left panel) and semilog scale (right panel). We observe a linear behavior on semilog scale for all momenta ($p = 0 - 0.9\pi$).

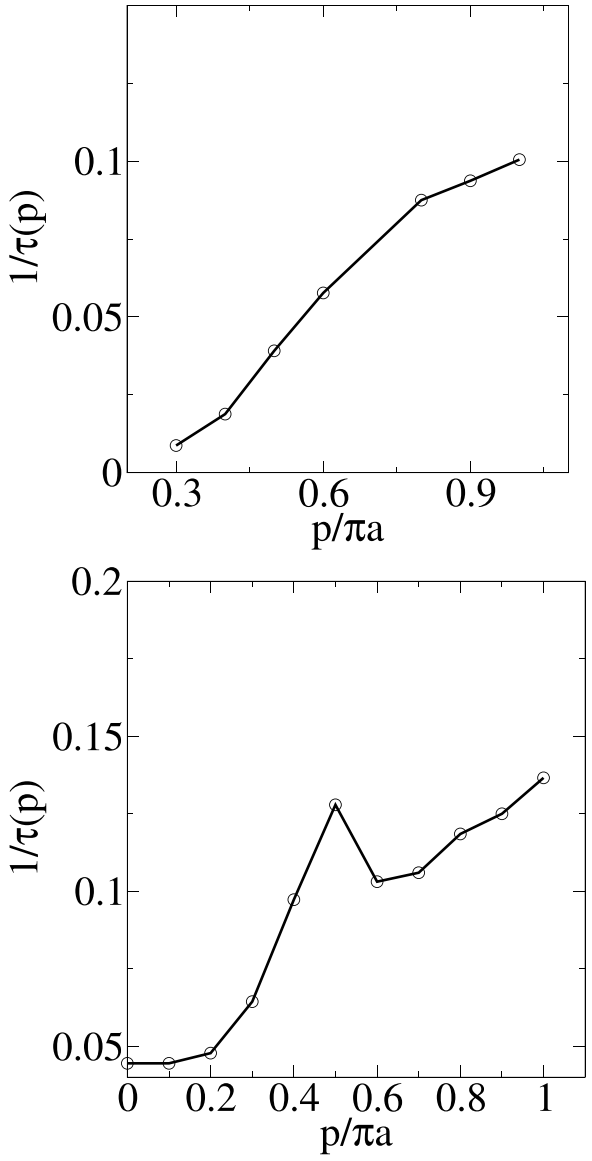

FIG. 9. Inverse lifetime of the impurity in both symmetric (upper panel) and antisymmetric (lower panel) sectors as a function of momentum at $t_b = 1$, $t_\perp = 1$, $t_{\rm imp} = 1$, $t_{\perp{\rm imp}} = 3$, and $U = 1.0$.

$p,\ t_{\perp{\rm imp}}$	$\lvert G_s(p,t)\rvert$	$\lvert G_a(p,t)\rvert$
$p = 0,\ 2t_{\perp{\rm imp}} > \frac{\Delta_a\sqrt{2u_a\pi}}{\sqrt{K_a}}$	Power-law	Exponential
$p = 0,\ 2t_{\perp{\rm imp}} < \frac{\Delta_a\sqrt{2u_a\pi}}{\sqrt{K_a}}$	Power-law	Power-law
$p \le \frac{u_s}{2t_{\rm imp}a^2},\ 2t_{\perp{\rm imp}} > \frac{\Delta_a\sqrt{2u_a\pi}}{\sqrt{K_a}}$	Power-law	Exponential
$p > \frac{u_s}{2t_{\rm imp}a^2},\ 2t_{\perp{\rm imp}} > \frac{\Delta_a\sqrt{2u_a\pi}}{\sqrt{K_a}}$	Exponential	Exponential

FIG. 10. Summary of the nature of $G_s(p,t)$ and $G_a(p,t)$ for different momenta at small impurity-bath interaction.

bath. In our LCE results, we find that Green's function of the impurity in the symmetric sector decays as a power law. In contrast, in the antisymmetric sector, it decays exponentially for $2t_{\perp{\rm imp}} > \Delta_a\sqrt{2u_a\pi}/\sqrt{K_a}$ and as a power law for $2t_{\perp{\rm imp}} < \Delta_a\sqrt{2u_a\pi}/\sqrt{K_a}$; the latter case is an emergent effect of the gap in the bath and transverse tunneling of the impurity on the dynamics of the impurity. In order to explore the dynamics of impurities across a wide range of parameters, we have conducted a t-DMRG simulation. For weak coupling, both numerical and analytical results show an excellent agreement, as depicted in Figs. 3 and 4.

The transverse tunneling of the impurity is the main ingredient in the exponential decay of the Green's function of the impurity in the antisymmetric mode, while for the Green's function in the symmetric mode, the power-law exponent does not depend on the transverse tunneling of the impurity.

Now, let us turn to the infinite interaction limit between the impurity and the bath. We find that the Green's function in the symmetric sector decays as a power law at zero momentum, which is similar to the one observed in the impurity dynamics in a 1D bath and two-leg ladder bath.

However, the power-law exponent increases with the tunneling amplitude of the impurity, which is in contrast to the behavior observed at small U, where the exponent does not depend on $t_{\perp{\rm imp}}$. We find that for small $t_{\perp{\rm imp}}$, the power-law exponent is the same as that observed in 1D motion in the ladder bath [19], but for a larger value, the power-law exponent is equal to that observed in the 1D bath [31]. As a function of $t_{\perp{\rm imp}}$, we observe that the impurity dynamics exhibits a dimensional crossover from ladder to 1D bath. For large transverse tunneling, one can understand that the impurity will energetically favor the symmetric mode of the impurity, and it would be hard to excite the impurity from symmetric to antisymmetric mode, and vice versa. Hence, the impurity effectively moves in a gapless 1D bath formed by the ladder's symmetric mode. This description contradicts our common understanding that in a ladder the power-law exponent should be smaller than that of 1D motion in the ladder [19].

It will be interesting to investigate how the dynamics of the impurity behaves with increasing number of legs and this needs a further study.

Our findings also suggest that the impurity in the symmetric sector at the zero momentum in the ladder can be viewed as an x-ray edge problem [9]. The Green's function in the x-ray edge problem has similar behavior as the Green's function of the symmetric mode at zero momentum. Of course in this case, contrarily to the historical x-ray edge problem, the impurity can move. At zero longitudinal tunneling of the impurity, the impurity-ladder problem can be mapped into a spin-boson problem [4] and by using an unitary transformation it can also be mapped into a Kondo problem [35]. The impurity-ladder problem can be viewed as a quantum simulator for the spin-boson model and Kondo problem.

Now, we finally turn to the case of finite momentum. For small interaction and small momentum, the Green's functions in the symmetric mode of the impurity decay as a power law, which are shown in the upper panel of Fig. 7. Beyond a critical momentum p^*, the Green's function is depicted in the lower panel of Fig. 7; it decays exponentially, and the impurity enters into a QP regime that is very similar to that observed in

the 1D motion of an impurity in a one-dimensional bath and in a two-leg bosonic ladder when $t_{\perp\text{imp}}$ is zero. The critical momentum is precisely equal to that of 1D motion of an impurity in a ladder and in a 1D bath. The Green's functions of the impurity in the antisymmetric mode are depicted in Fig. 8, and they always decay exponentially for all momenta, and the impurity in the antisymmetric mode always behaves like a QP.

VI. CONCLUSION AND PERSPECTIVES

We have studied the dynamics of an impurity in a reservoir of hardcore bosons moving in a two-leg ladder where the impurity may tunnel in both transverse and horizontal directions. We have computed the Green's function of the impurity for different momenta in order to understand the dynamics of the impurity. We use both analytical and numerical approaches, where the latter are comprised of the time-dependent DMRG.

The transverse tunneling of the impurity and gap in the bath drastically affects the impurity dynamics. Even in the antisymmetric sector, the impurity Green's function exhibits a power-law behavior for sufficiently small transverse tunneling of the impurity compared to the gap in the bath. For large impurity-bath coupling, the impurity dynamics exhibits a crossover from dynamics in a ladder bath to a 1D bath.

The system we have studied can be tested experimentally in the context of circuit QED [36,37] and cold atoms. When the impurity moves only in the transverse direction, the impurity acts like a two-level system that is analogous to a superconducting qubit, and the two-leg ladder bath acts like a one-dimensinal waveguide, and the impurity-reservoir interaction is the equivalent of the standard qubit-waveguide coupling. The bosonic ladder has been realized experimentally in ultracold gases [38,39] and atom chips [40]. The impurity dynamics in one-dimensional bath has been investigated experimentally using ultracold gases [22–25]. Combination of these aspects and ongoing experimental advancement in the ultracold gases could provide the ideal testbed for our findings in the near future.

ACKNOWLEDGMENTS

Calculations were performed using the Matrix Product Toolkit [41]. We thank N. Laflorencie and G. Roux for providing us with the precise numerical value for the TLL parameters of the ladder of publication [32]. This work was supported in part by the Swiss National Science Foundation under Grant No. 200020-219400, ERC Starting Grant from the European Union's Horizon 2020 Research and Innovation Programme under Grant Agreement No. 758935, and the UK's Engineering and Physical Sciences Research Council (EPSRC; Grant No. EP/W022982/1).

APPENDIX: GREEN'S FUNCTION OF THE MOBILE IMPURITY IN THE TWO-LEG BOSONIC LADDER

We have shown in the main text (see Sec. III) that for small interaction U between the impurity and the ladder bath, the impurity effectively coupled to the forward scattering terms of the gapped and gapless modes of the bath.

In this section, we give an LCE expression [30] of the Green's function of the impurity. We express $\cos(\sqrt{2}\theta_a) = 1 - \theta_a^2$ and use the continuity equation:

$$\nabla\phi_a(q,t) = \frac{\partial\theta_a(q,t)}{\partial t}. \tag{A1}$$

The impurity-bath Hamiltonian is expressed as

$$H = H_s + H_a + H_{\text{imp}} + H_{\text{coup}}, \tag{A2}$$

where H_s, H_a, H_{imp}, and H_{coup} are the symmetric mode and antisymmetric mode of the bath, the impurity Hamiltonian, and the coupling between the impurity and the bath, respectively, and these terms in bosonized language are expressed as

$$\begin{aligned}
H_s &= \sum_q u_s|q| b^\dagger_{s,q} b_{s,q},\\
H_a &= \frac{1}{2\pi}\int dx\left[u_a K_a(\partial_x\theta_a)^2 + \frac{u_a}{K_a}(\partial_x\phi_a)^2\right]\\
&\quad + \Delta_a^2\int dx\theta_a(x)^2,\\
H_{\text{coup}} &= \sum_{q,k}\Big[V(q)(d^\dagger_{s,k+q}d_{s,k} + d^\dagger_{a,k+q}d_{a,k})(b_{s,q} + b^\dagger_{s,-q})\\
&\quad + \tilde{U}(d^\dagger_{a,k+q}d_{s,k} + d^\dagger_{s,k+q}d_{a,k})\frac{\partial\theta_a(q,t)}{\partial t}\Big],\\
H_{\text{imp}} &= \sum_q \epsilon_s(q) d^\dagger_{s,q}d_{sq} + \epsilon_a(q) d^\dagger_{a,q}d_{a,q},
\end{aligned} \tag{A3}$$

where $\tilde{U} = -U/\sqrt{2}\pi$, $b^\dagger$ and $d^\dagger$ are the creation operators for the bath in the bosonized language and the impurity, respectively, $\epsilon_a(p) = -2t_{\text{imp}}\cos(p) + t_{\perp\text{imp}}$, and $\epsilon_s(p) = -2t_{\text{imp}}\cos(p) - t_{\perp\text{imp}}$. Δ_a is the gap in the antisymmetric mode of the bath. The coupling term $V(q)$ can be expressed as

$$V(q) = \frac{U}{\sqrt{2}}\sqrt{\frac{K_s|q|}{2\pi L}}\exp\Big(-\frac{|q|}{2q_c}\Big). \tag{A4}$$

The Green's functions of the impurity in symmetric and antisymmetric sectors are defined by

$$\begin{aligned}
G_s(p,t) &= -i\langle d_{s,p}(t)d^\dagger_{s,p}(0)\rangle,\\
G_a(p,t) &= -i\langle d_{a,p}(t)d^\dagger_{a,p}(0)\rangle.
\end{aligned} \tag{A5}$$

By using LCE, Eq. (A5) can be written as

$$\begin{aligned}
G_s(p,t) &= -ie^{-i\epsilon_s(p)t}e^{F_{2s}(p,t)},\\
G_a(p,t) &= -ie^{-i\epsilon_a(p)t}e^{F_{2a}(p,t)},
\end{aligned} \tag{A6}$$

where $F_{2,s/a}(p,t)$ is defined as

$$F_{2s/a}(p,t) = e^{i\epsilon_{s/a}(p)t}W_{2s/a}(p,t). \tag{A7}$$

$W_{2s/a}(p,t)$ is given by

$$\begin{aligned}
W_{2s/a}(p,t) = -\frac{1}{2}\int_0^t dt_1\int_0^t dt_2\langle T_t d_{s/a,p}(t)H_{\text{coup}}(t_1)\\
\times H_{\text{coup}}(t_2)d^\dagger_{s/a,p}(0)\rangle.
\end{aligned} \tag{A8}$$

By employing the Wick's theorem, $W_{2a}(p,t)$ can be expressed as

$$W_{2a}(p,t) = -\sum_q \int_0^t dt_1 \int_0^t dt_2 \Theta(t-t_1)\Theta(t_1-t_2)\Theta(t_2)\Bigg[V(q)^2 e^{-i\epsilon_a(p)(t-t_1)} e^{-i\epsilon_a(p+q)(t_1-t_2)} e^{-i\epsilon_a(p)t_2} e^{-i(u_s|q|(t_1-t_2))} + \frac{U^2}{4\pi}\sqrt{K_a^2q^2 + \frac{2\pi\Delta_a^2 K_a}{u_a}} e^{-i\epsilon_a(p)(t-t_1)} e^{-i\epsilon_s(p+q)(t_1-t_2)} e^{-i\epsilon_a(p)t_2} e^{-i\left(\sqrt{u_a^2q^2+\frac{2\pi\Delta_a^2 u_a}{K_a}}(t_1-t_2)\right)}\Bigg], \tag{A9}$$

where $\Theta(t)$ is a step function, which is 0 for $t<0$ and 1 for $t>0$. $\Theta(t)$ changes the limit of integration of t_2 and t_1, and $F_{2a}(p,t)$ is modified as

$$F_{2a}(p,t) = -\sum_q \int_0^t dt_1 \int_0^{t_1} dt_2 \Bigg[V(q)^2 e^{i\epsilon_a(p)t_1} e^{-i\epsilon_a(p+q)(t_1-t_2)} e^{-i\epsilon_a(p)t_2} e^{-i(u_s|q|(t_1-t_2))} + \frac{U^2}{4\pi}\sqrt{K_a^2q^2 + \frac{2\pi\Delta_a^2 K_a}{u_a}} e^{i\epsilon_a(p)t_1} e^{-i\epsilon_s(p+q)(t_1-t_2)} e^{-i\epsilon_a(p)t_2} e^{-i\left(\sqrt{u_a^2q^2+(2\pi\Delta_a^2 u_a/K_a)}(t_1-t_2)\right)}\Bigg]. \tag{A10}$$

We can simplify Eq. (A10) as

$$F_{2a}(p,t) = -\sum_q \int du \int_0^t dt_1 \int_0^{t_1} dt_2 \Bigg[V(q)^2 e^{it_1u} e^{-it_2u}\delta(u-\epsilon(p)+\epsilon(p+q)+u_s|q|) + \frac{U^2}{4\pi}\sqrt{K_a^2q^2 + \frac{2\pi\Delta_a^2 K_a}{u_a}} e^{-iut_1} e^{iut_2}\delta\left(u+\epsilon_a(p)-\epsilon_s(p+q)-\sqrt{u_a^2q^2+\frac{2\pi\Delta_a^2 u_a}{K_a}}\right)\Bigg]. \tag{A11}$$

Finally, we integrate over t_1 and t_2, and the real part of F_{2a} can be expressed as

$$\mathrm{Re}[F_{2a}(p,t)] = -\sum_q \int du \Bigg[V(q)^2 \frac{(1-\cos(ut))}{u^2}\delta(u-\epsilon(p)+\epsilon(p+q)+u_s|q|) + \frac{(1-\cos(tu))}{u^2}R_{2a}(u,p)\Bigg]. \tag{A12}$$

Similarly, one can show that

$$\begin{aligned}\mathrm{Re}[F_{2s}(p,t)] &= -\sum_q \int du \Bigg[V(q)^2\delta(u-\epsilon(p)+\epsilon(p+q)+u_s|q|))\frac{(1-\cos(ut))}{u^2} \\ &\quad + \frac{U^2}{4\pi}\sqrt{K_a^2q^2 + \frac{2\pi\Delta_a^2 K_a}{u_a}}\frac{(1-\cos(tu))}{u^2}\delta\left(u+\epsilon_s(p)-\epsilon_a(p+q)-\sqrt{u_a^2q^2+\frac{2\pi\Delta_a^2 u_a}{K_a}}\right)\Bigg], \\ &= -\int du\Bigg[\frac{(1-\cos(ut))}{u^2}R_1(u,p) + \frac{(1-\cos(tu))}{u^2}R_{2s}(u,p)\Bigg].\end{aligned} \tag{A13}$$

$R_1(u)$, R_{2a}, and R_{2s} are expressed as

$$R_1(u,p) = \frac{1}{2\pi}\int dq V(q)^2\delta(u-(\epsilon(p)-\epsilon(p+q)-u_s|q|)), \tag{A14}$$

$$R_{2a}(u,p) = \frac{U^2}{8\pi^2}\int dq\sqrt{K_a^2q^2+\frac{2\Delta_a^2K_a\pi}{u_a}}\delta\left(u+2t_{\perp imp}+\epsilon(p)-\epsilon(p+q)-\sqrt{u_a^2q^2+\frac{\Delta_a^2u_a2\pi}{K_a}}\right),$$

$$R_{2s}(u,p) = \frac{U^2}{8\pi^2}\int dq\sqrt{K_a^2q^2+\frac{2\Delta_a^2K_a\pi}{u_a}}\delta\left(u-2t_{\perp imp}+\epsilon(p)-\epsilon(p+q)-\sqrt{u_a^2q^2+\frac{\Delta_a^2u_a2\pi}{K_a}}\right). \tag{A15}$$

For small p, $\epsilon(p)\simeq t_{\mathrm{imp}}p^2$. $R_1(u,p)$ is computed in Refs. [19,31] for $[(p-(u_s/2t_{\mathrm{imp}})]<0, \wedge u<0$. However, the computation of $R_2(u,p)$ for an arbitrary p is difficult analytically, so we restrict at $p=0$. At $p=0$, R_1 is nonzero for $u<0$ can be expressed as

$$R_1(u,0)\propto u, \tag{A16}$$

and for $u > \tilde{\Delta} - 2t_{\perp\text{imp}}$,

$$R_{2a}(u,0) \propto A_2. \tag{A17}$$

Let us define $A_s(t)$ and $A_a(t)$ as

$$A_a(t) = -\frac{K_s U^2}{4\pi^2 u_s^2}\int_0^\infty du\left[\frac{1-\cos(ut)}{u}\right] + \int_{(\Delta_a\sqrt{2u_a\pi}/\sqrt{K_a})-2t_{\perp\text{imp}}}^\infty du\left[\frac{1-\cos(ut)}{u^2}A_2\right],$$
$$A_s(t) = -\frac{K_s U^2}{4\pi^2 u_s^2}\int_0^\infty du\left[\frac{1-\cos(ut)}{u}\right] + \int_{(\Delta_a\sqrt{2u_a\pi}/\sqrt{K_a})+2t_{\perp\text{imp}}}^\infty du\left[\frac{1-\cos(ut)}{u^2}R_{2s}(u,0)\right]. \tag{A18}$$

In the long-time limit, A_s and A_a can be expressed as

$$A_a(t) \simeq -A_2\pi t - \frac{K_s U^2}{4\pi^2 u_s^2}\log(t), \quad \text{if } 2t_{\perp\text{imp}} > \frac{\Delta_a\sqrt{2u_a\pi}}{\sqrt{K_a}}$$
$$\simeq -\frac{K_s U^2}{4\pi^2 u_s^2}\log(t), \quad \text{if } 2t_{\perp\text{imp}} < \frac{\Delta_a\sqrt{2u_a\pi}}{\sqrt{K_a}},$$
$$A_s(t) \simeq -\frac{K_s U^2}{4\pi^2 u_s^2}\log(t), \tag{A19}$$

where $\Theta(x)$ is a Heaviside step function defined as $\Theta(x) = 1$ for $x > 0$ and 0 for $x < 0$, and A_2 is expressed as

$$A_2 \simeq \frac{U^2 K_a}{4u_a\pi^2}\frac{\left(u_a^2 q_-^2 + \tilde{\Delta}^2\right)}{q_-\left(2t_{\text{imp}}\sqrt{u_a^2 q_-^2 + \tilde{\Delta}^2} + u_a^2\right)}, \tag{A20}$$

and $\tilde{\Delta}$ and q_- are expressed as

$$\tilde{\Delta} = \frac{\Delta_a\sqrt{u_a 2\pi}}{\sqrt{K_a}},$$
$$q_- = \sqrt{\frac{2t_{\perp\text{imp}}}{t_{\text{imp}}} + \frac{u_a^2}{2t_{\text{imp}}^2} - \sqrt{\left(\frac{2t_{\perp\text{imp}}}{t_{\text{imp}}} + \frac{u_a^2}{2t_{\text{imp}}{}^2}\right)^2 - \frac{\left(4t_{\perp\text{imp}}^2 - \tilde{\Delta}^2\right)}{t_{\text{imp}}^2}}}. \tag{A21}$$

By using Eqs. (A12), (A13), (A18), and (A19), the final expression of F_{2s}, F_{2a} in long-time limit is given by

$$\text{Re}[F_{2a}(0,t)] \simeq A_a(t), \tag{A22}$$

$$\text{Re}[F_{2s}(0,t)] \simeq A_s(t), \tag{A23}$$

leading to the Green's function decay as

$$|G_a(0,t)| = e^{A_a(t)}, \tag{A24}$$

$$|G_s(p,t)| = e^{A_s(t)}. \tag{A25}$$

[1] R. P. Feynman, Slow electrons in a polar crystal, Phys. Rev. **97**, 660 (1955).

[2] R. P. Feynman, *Statistical Mechanics* (Benjamin, Reading, MA, 1972).

[3] A. O. Caldeira and A. J. Leggett, Quantum tunnelling in a dissipative system, Ann. Phys. **149**, 374 (1983).

[4] A. J. Leggett, S. Chackravarty, A. T. Dorsy, M. P. A. Fisher, A. Garg, and W. Zwerger, Dynamics of the dissipative two-state system, Rev. Mod. Phys. **59**, 1 (1987).

[5] C. Franchini, M. Reticcioli, M. Setvin, and U. Diebold, Polarons in materials, Nat. Rev. Mater. **6**, 560 (2021).

[6] T.-L. Dao, A. Georges, J. Dalibard, C. Salomon, and I. Carusotto, Measuring the one-particle excitations of ultracold fermionic atoms by stimulated Raman spectroscopy, Phys. Rev. Lett. **98**, 240402 (2007).

[7] M. G. Skou, T. G. Skov, N. B. Jørgensen, K. K. Nielsen, A. Camacho-Guardian, T. Pohl, G. M. Bruun, and J. J. Arlt, Non-equilibrium quantum dynamics and formation of the Bose polaron, Nat. Phys. **17**, 731 (2021).

[8] P. W. Anderson, Infrared catastrophe in Fermi gases with local scattering potentials, Phys. Rev. Lett. **18**, 1049 (1967).

[9] T. Giamarchi, *Quantum Physics in One Dimension* (Oxford University Press, New York, 2003), Vol. 121.

[10] M. Zvonarev, V. V. Cheianov, and T. Giamarchi, Spin dynamics in a one-dimensional ferromagnetic Bose gas, Phys. Rev. Lett. **99**, 240404 (2007).

[11] A. Kamenev and L. Glazman, Dynamics of a one-dimensional spinor Bose liquid: A phenomenological approach, Phys. Rev. A **80**, 011603(R) (2009).
[12] A. Matveev and A. Furusaki, Spectral functions of strongly interacting isospin-1/2 Bosons in one dimension, Phys. Rev. Lett. **101**, 170403 (2008).
[13] M. Schecter, A. Kamenev, D. Gangardt, and A. Lamacraft, Critical velocity of a mobile impurity in one-dimensional quantum liquids, Phys. Rev. Lett. **108**, 207001 (2012).
[14] A. Lamacraft, Dispersion relation and spectral function of an impurity in a one-dimensional quantum liquid, Phys. Rev. B **79**, 241105 (2009).
[15] M. B. Zvonarev, V. V. Cheianov, and T. Giamarchi, Dynamical properties of the one-dimensional spin-1/2 Bose-Hubbard model near a Mott-insulator to ferromagnetic-liquid transition, Phys. Rev. Lett. **103**, 110401 (2009).
[16] M. B. Zvonarev, V. V. Cheianov, and T. Giamarchi, Edge exponent in the dynamic spin structure factor of the Yang-Gaudin model, Phys. Rev. B **80**, 201102(R) (2009).
[17] E. Müller-Hartmann, T. V. Ramakrishnan, and G. Toulouse, Localized dynamic perturbations in metals, Phys. Rev. B **3**, 1102 (1971).
[18] A. Rosch and T. Kopp, Heavy particle in a *d*-dimensional fermionic bath: A strong coupling approach, Phys. Rev. Lett. **75**, 1988 (1995).
[19] N. A. Kamar, A. Kantian, and T. Giamarchi, Dynamics of a mobile impurity in a two-leg bosonic ladder, Phys. Rev. A **100**, 023614 (2019).
[20] M. Stefanini, M. Capone, and A. Silva, Motion of an impurity in a two-leg ladder, Phys. Rev. B **103**, 094310 (2021).
[21] M. Stefanini, M. Capone, and A. Silva, Full view on the dynamics of an impurity coupled to two one-dimensional baths, Phys. Rev. B **107**, 184316 (2023).
[22] S. Palzer, C. Zipkes, C. Sias, and M. Köhl, Quantum transport through a Tonks-Girardeau gas, Phys. Rev. Lett. **103**, 150601 (2009).
[23] J. Catani, G. Lamporesi, D. Naik, M. Gring, M. Inguscio, F. Minardi, A. Kantian, and T. Giamarchi, Quantum dynamics of impurities in a one-dimensional Bose gas, Phys. Rev. A **85**, 023623 (2012).
[24] T. Fukuhara, A. Kantian, M. Endres, M. Cheneau, P. Schauß, S. Hild, D. Bellem, U. Schollwöck, T. Giamarchi, C. Gross *et al.*, Quantum dynamics of a mobile spin impurity, Nat. Phys. **9**, 235 (2013).
[25] F. Meinert, M. Knap, E. Kirilov, K. Jag-Lauber, M. B. Zvonarev, E. Demler, and H.-C. Nägerl, Bloch oscillations in the absence of a lattice, Science **356**, 945 (2017).
[26] T. Kopp, A. Ruckenstein, and S. Schmitt-Rink, Single spin flip in the Nagaoka state: Problems with the Gutzwiller wave function, Phys. Rev. B **42**, 6850 (1990).
[27] S. R. White, Density matrix formulation for quantum renormalization groups, Phys. Rev. Lett. **69**, 2863 (1992).
[28] U. Schollwöck, The density-matrix renormalization group, Rev. Mod. Phys. **77**, 259 (2005).
[29] F. D. M. Haldane, Demonstration of the "Luttinger liquid" character of Bethe-ansatz-soluble models of 1-D quantum fluids, Phys. Lett. A **81**, 153 (1981).
[30] G. D. Mahan, *Many-Particle Physics* (Springer Science & Business Media, New York, 2000).
[31] A. Kantian, U. Schollwöck, and T. Giamarchi, Competing regimes of motion of 1d mobile impurities, Phys. Rev. Lett. **113**, 070601 (2014).
[32] F. Crépin, N. Laflorencie, G. Roux, and P. Simon, Phase diagram of hard-core bosons on clean and disordered two-leg ladders: Mott insulator–Luttinger liquid–Bose glass, Phys. Rev. B **84**, 054517 (2011).
[33] U. Schollwöck, The density-matrix renormalization group in the age of matrix product states, Ann. Phys. **326**, 96 (2011).
[34] N. A. Kamar, Quantum dynamics in one-dimensional and two-leg ladder systems, Ph.D. thesis, University of Geneva, 2019.
[35] M. Blume, V. J. Emery, and A. Luther, Spin-boson systems: One-dimensional equivalents and the Kondo problem, Phys. Rev. Lett. **25**, 450 (1970).
[36] P. Forn-Díaz, J. J. García-Ripoll, B. Peropadre, J.-L. Orgiazzi, M. Yurtalan, R. Belyansky, C. M. Wilson, and A. Lupascu, Ultrastrong coupling of a single artificial atom to an electromagnetic continuum in the nonperturbative regime, Nat. Phys. **13**, 39 (2017).
[37] L. Magazzù, P. Forn-Díaz, R. Belyansky, J.-L. Orgiazzi, M. Yurtalan, M. R. Otto, A. Lupascu, C. Wilson, and M. Grifoni, Probing the strongly driven spin-boson model in a superconducting quantum circuit, Nat. Commun. **9**, 1403 (2018).
[38] M. Atala, M. Aidelsburger, M. Lohse, J. T. Barreiro, B. Paredes, and I. Bloch, Observation of chiral currents with ultracold atoms in bosonic ladders, Nat. Phys. **10**, 588 (2014).
[39] T. Stöferle, H. Moritz, C. Schori, M. Köhl, and T. Esslinger, Transition from a strongly interacting 1D superfluid to a Mott insulator, Phys. Rev. Lett. **92**, 130403 (2004).
[40] S. Hofferberth, I. Lesanovsky, T. Schumm, A. Imambekov, V. Gritsev, E. Demler, and J. Schmiedmayer, Probing quantum and thermal noise in an interacting many-body system, Nat. Phys. **4**, 489 (2008).
[41] https://people.smp.uq.edu.au/IanMcCulloch/mptoolkit/.